Received: 26 July 2018 | Revised: 17 September 2018 | Accepted: 23 September 2018

DOI: 10.1002/tox.22665

WILEY ENVIRONMENTAL TOXICOLOGY

RESEARCH ARTICLE

Mechanisms involved in inflammatory pulmonary fibrosis induced by lunar dust simulant in rats

Yan Sun[1,2,3] | Jinguo Liu[3] | Xiaoping Zhang[2,4] | Xiongyao Li[5] | Baichu Zhou[1] | Zengjing Lv[1]

[1]College of Basic Medical Sciences, Shenyang Medical College, Shenyang, China

[2]Lunar and Planetary Science Laboratory, MUST-Partner Laboratory of Key Laboratory of Lunar and Deep Space Exploration, CAS, Macau, China

[3]State Key Laboratory of Robotics, Shenyang Institute of Automation, Chinese Academy of Sciences, Shenyang, China

[4]Lunar and Planetary Science Laboratory, Macau University of Science and Technology, Macau, China

[5]Center for Lunar and Planetary Sciences, Institute of Geochemistry, Chinese Academy of Sciences, Guiyang, China

Correspondence
Yan Sun, College of Basic Medical Sciences, Shenyang Medical College, Shenyang 110034, China.
Email: sunyan@symc.edu.cn
and
Jinguo Liu, State Key Laboratory of Robotics, Shenyang Institute of Automation, Chinese Academy of Sciences, Shenyang 110016, China.
Email: liujinguo@sia.cn

Funding information
Doctoral Scientific Research Fund of Liaoning Provincial Science and Technology Department, Grant/Award Number: 20170520437; National Natural Science Foundation of China, Grant/Award Number: 51775541; Open Projects Funding of Lunar and Planetary Science Laboratory, MUST - Partner Laboratory of Key Laboratory of Lunar and Deep Space Exploration, CAS, Grant/Award Number: 119/2017/A3; Science and Technology Development Fund (FDCT) of Macau, Grant/Award Number: 020/2014/A1; Science and Technology Research Fund of Shenyang Medical College, Grant/Award Number: 20171020

Abstract

Lunar dust is one of the biggest risk factors in the future manned exploration mission. Much is not known about the pulmonary toxicity of lunar dust. The aim of this study was to evaluate the lung inflammation and oxidative stress induced by subacute exposure to lunar dust stimulant (LDS) in rats. Wistar rats were intratracheally administered LDS, twice a week for 3 weeks. Inflammatory cell counting and cytokine assays using bronchoalveolar lavage fluid (BALF) were performed. Lung tissues were processed for histopathological examination and immunohistochemical staining. Biomarkers of oxidative stress and genes and proteins related to inflammation and fibrosis in lung tissue were also determined. The neutrophil count in the BALF of LDS-exposed groups was higher than that in controls ($P < .05$). LDS caused a significant increase in some of biochemical indicators and proinflammatory factors levels in BALF compared with control group. The normal balance between oxidation and antioxidation was broken by LDS. Pathological characteristics of lung tissue and immunohistochemical results for α-smooth muscle actin (α-SMA) indicated that inflammatory response was an extremely important passage to pulmonary fibrosis. Real-time PCR analysis showed elevated levels of nitric oxide synthase (NOS) and nicotinamide adenine dinucleotide phosphate oxidase (NOX) mRNA in the lungs ($P < .05$). Western blotting results were consistent with immunohistochemistry and qPCR results. These results indicate that inhalation of lunar dust may cause inflammatory pulmonary fibrosis. NOX4 may be a key potential therapeutic target for inflammatory injury and fibrosis in the lung.

KEYWORDS

fibrosis, inflammation, lunar dust, lung, oxidative stress

1 | INTRODUCTION

The Apollo lunar exploration has shown that diffusion of lunar dust particles can cause visual obstruction, dust pollution, adhesion, inhalation, physiological effects, and so on.[1,2] The projected duration of future lunar inhabitation is longer than that of the Apollo astronauts, and presence of lunar dust poses one of the biggest challenges for such kind of future missions. The living quarters could be contaminated with dust present on spacesuits or hardware. Dust exposure and inhalation could have a wide range of toxic effects on lunar explorers. Thus, there is a need for assessing the health risks of human exposure to lunar dust. The present study was carried out to acquire such information on toxicity of airborne lunar dust.

In general, lunar regolith contains about 20% dust particles with diameter less than 20 μm, and 1%-2% fine dust particles with diameter less than 3 μm.[3] Lunar dust is mainly composed of glass (≥50%),

plagioclase, pyroxene, olivine, ilmenite, nanophase Fe^0, and so on.[4] As a unique component of the lunar dust, nanometallic iron is formed by striking the moon resulting in vaporizing and deposition of dust particles.[5] Cosmic and solar radiations charge the lunar surface components[6] (NASA, 2009); charges build up to levels which are high enough to repel submicron particles (0.1 mm) as high as 100 km (62 miles or ~330 000 ft) and could remain above the low gravity and airless lunar surface for long periods.[7] In amicro-/hypo-gravity environment, the risk of inhalation of dust is increased due to reduced gravity-induced sedimentation.[8]

The formation, composition, and physical properties of lunar dust are not yet characterized with respect to human health. While the physical and chemical determinants of dust toxicity for materials such as asbestos, quartz, volcanic ashes, and urban particulate matter have been the focus of substantial research, lunar dust toxicity may differ significantly due to its unique properties. NASA scientists implemented a series of studies to study the effects of lunar dust exposure. Cellular and biochemical markers of toxicity and lung histopathology were assayed in bronchoalveolar lavage fluid (BALF).The results showed that exposure to lunar dust induced lung inflammation.[9,10] We obtained a similar conclusion in a previous study.[11] Lunar dust was moderately toxic. It was more toxic than TiO_2 but less toxic than quartz.[12,13] Although the above studies have provided useful insights on induction of pulmonary toxicity by lunar dust, there are major knowledge gaps that prevent an accurate assessment of lunar dust toxicity, especially with respect to the mechanism of lung toxicity.

To obtain new insights on the mechanism of lung toxicity caused by lunar dust, we investigated the effects of CLDS-i (a standard lunar dust simulant) exposure on the rats for 3 weeks. The lung inflammatory effects, oxidative stress response, and the key factors in pulmonary fibrosis were assessed. The results showed that inflammation and oxidative stress are important mechanisms of lung injury caused by LDS and lead to pulmonary fibrosis. Nicotinamide adenine dinucleotide phosphate oxidase 4 (NOX4) may be a potential therapeutic target in this respect.

2 | MATERIALS AND METHODS

2.1 | Animal protocol

Male Wistar rats (190-220 g) were purchased from Liaoning Changsheng Biotechnology Co. Ltd (Animals License number: SCXK [Liao] 2010-0001). They were kept in polycarbonate cages (equipped with HEPA air filter) for 1 week. Next, all the rats were equally divided into four groups: normal saline group (control), LDS low-dose group, LDS middle-dose group, and LDS high-dose group. Each animal group had six rats.

All rats were exposed to LDS twice per week for 3 weeks. The intratracheal instillation method was used for the administration of the dust samples. The high-dose, middle-dose, and low-dose groups were injected with 3.15, 1.05, and 0.35 mg of LDS, in a 1 mL perfusion volume, respectively. Simultaneously, the control groups were injected with the same amount of normal saline. After intratracheal instillation of the preheated dust suspension (saline solution), the rats were rotated several times to evenly distribute the liquid. The rats were anesthetized with chloral hydrate (320 mg/kg, i.p.) before instillation of LDS or saline. Then the rats were killed after 24 hours of the last intratracheal instillation for the next step of the experiment. All the animal studies were approved by the Ethics Committee of Animal Care and Experimentation of the National Institute for Environmental Studies, China.

2.2 | Lunar dust simulant

CLDS-i with smaller particle size is one of series of simulated lunar dust samples just like CAS-1 simulants which we used.[11] It has the similar chemical composition, mineral composition, grain size, grain shape, and nanophase metal iron composition like real lunar dust. The CLDS-i with a median particle size about 500 nm contains approximately 75% v/v glass and a little amount of nanophase iron (np-Fe^0). Detailed description and comparison have been described by Tang et al.[14] The CLDS-i particles also have complicated shapes and sharp edges.[14] CLDS-i are obtained by ball milling, magnetic screening under a high intensity magnetic field, star milling, ultrasonic breaking, and bombardment. Most of CLDS-i particles with diameter size under 1μm could be obtained using this protocol.

2.3 | Cell differential counts and biochemical analysis

After administering the dust suspension, the rats were anesthetized with chloral hydrate (320 mg/kg, i.p.) and then laid on their backs on a platform. Immediately they were exsanguinated by the abdominal aorta. After that, the left main bronchus was temporarily closed with a hemostatic clamp and 3 mL of cold sterile saline was instilled to lavage their lungs three times.[15] BALF was collected in 5 mL sterile centrifuge tubes and placed on ice. The samples were centrifuged (1500 rpm for 10 minutes at 4°C), and cells were collected for cell counts and differentiation by a hemocytometer. The supernatants were stored at −80°C for further analysis of biochemical indicators.

The cell samples collected from the centrifuge were mixed with 200 μL of saline. Next, 20 μL of this suspension was dropped onto a clean glass slide. After the drop dried, 100 cells were stained with Giemsa for analysis of cellular differentiation of macrophages, neutrophils, and lymphocytes. The biochemical parameters, including lactate dehydrogenase (LDH), alkaline phosphatase (AKP), albumin (ALB), and total protein (TP) in the supernatant, were detected by the automatic biochemical analyzer (P800, Roche, Shanghai, China) in the clinical laboratory of the Affiliated Center Hospital of Shengyang Medical College. Interleukin-6 (IL-6) and tumor necrosis factor alpha (TNF-α) were analyzed using ELISA kits (ABclonal Technology, Wuhan, China). All the biomarkers were analyzed three times to obtain an average value.

2.4 | Histopathological examination and immunohistochemical test

Some parts of the left lungs of rats were used as samples (unwashed), and were placed in 10% paraformaldehyde solution. After fixation, ethanol gradient dehydration, xylene transparent treatment,

sectioning of the paraffin-embedded tissues at 5 μm, and staining with Hematoxylin and Eosin (H&E) and Masson's trichrome was done.

Immunohistochemical analysis was also performed to determine levels of Nox4 and α-smooth muscle actin (α-SMA). The pathological changes in lung tissues were observed using a DM750 pathological microscope (Leica, Germany). Image J software (National Institutes of Health, Bethesda, MD, USA) was used to evaluate the percentage of blue-colored trichrome-positive stained and the positive immunostained lung tissue area.

2.5 | Preparation of lung homogenates and biochemical analysis

The rest of the left lung, except for that used for histopathological examination, was separated into two parts. One part was homogenized in ice-cold saline with glass-homogenizer. The homogenate concentration was 10%. Then the homogenate was centrifuged (3000 rpm for 10 minutes at 4°C). The supernatant was collected and stored at −80°C for detection of biomarkers of oxidative stress. The activities of glutathione peroxidase (GSH-Px), superoxide dismutase (SOD), and malondialdehyde (MDA) were determined by the commercial colorimetric assay kit (Nanjing Jiancheng Bioengineering Institute, Jiangsu, China). The other part was snap frozen in liquid nitrogen, then stored at −80°C for RNA analysis.

2.6 | RNA extraction and real-time PCR

The frozen lung samples were homogenized in TRIzol reagent (Invitrogen, CA, USA), and total RNA was extracted according to the manufacturer's instructions. Isolated RNA was converted to cDNA using Promega reverse transcription reagent (Madison, Wisconsin, USA) according to the manufacturer's instructions. qPCR reactions were performed in an ABI PRISM 7500 system. The amplification of specific PCR products was detected using SYBR Green PCR Master MixReagent (Applied Biosystems). Expression levels of endothelial nitric oxide synthase (eNOS), inducible nitric oxide synthase (iNOS), and nicotinamide adenine dinucleotide phosphate oxidase (NADPH oxidase, NOX) 2 and 4 were measured using the following primers (Invitrogen, CA, USA): iNOS forward, 5′-AATGGTTTCCCCCAG TTCCTCACT-3′; iNOS anti-sense, 5′-CTCTCCATTGCCCCAGTTTTTG A-3′; eNOS forward, 5′-CGGTACTACTCTGTCAGCTCAGC-3′ and reverse, 5′-CATCCTGGGTTCTGTATGCC-3′; GAPDH forward, 5′-CAAGTTCAACGGCACAGTCA-3′ and reverse, 5′-CACCCCATTTG ATGTTAGCG-3′;[16] Nox2 forward, 5′-CCCTTTGGTACAGCCAGTG AAGAT-3′ and reverse, 5′-CAATCCCAGCTCCCACTAACATCA-3′; Nox4 forward, 5′-GGATCACAGAAGGTCCCTAGCAG-3′ and reverse, 5′-GCAGCTACATGCACACCTGAGAA-3′;[17] β-actin forward, 5′-CACT ATCGGCAATGAGCGGTTCC-3′ and reverse, 5′-CTGTGTTGGCAT AGAGGTCTTTACGG-3′.[16] For iNOS and eNOS, the data was normalized to the housekeeping gene GAPDH. For NOX2 and NOX4, the data was normalized to the housekeeping gene β-actin. Data were analyzed using the comparative threshold cycle (CT) method and each sample was analyzed in duplicate.

2.7 | Western blotting analysis

The frozen lung samples were homogenized in RIPA protein lysate (containing 10% PMSF) (Wanleibio, Liaoning, China). Then, the homogenate was centrifuged at 12 000*g*, at 4°C for 30 minutes and supernatant was collected. Subsequently, protein levels were estimated by Bradford protein assay (Bio-Rad Hercules, CA, USA). Total proteins were electrophoresed in SDS-PAGE system and the gel bands were electrophoretically transferred to polyvinylidene fluoride (PVDF) membranes. The membranes were blocked with 5% skim milk for 1 hour. Immunoblotting was performed using antibodies against rat α-SMA (Wanleibio, Liaoning, China), NOX4 (Bio-Rad Hercules, CA, USA) and β-actin (Santa Cruz Biotechnology, Santa Cruz, CA) at the manufacturer's recommended dilutions. Protein signals were finally detected using enhanced chemiluminescence (ECL) reagent (SuperSignal Western Pico Chemiluminescent Substrate, Pierce, USA).

2.8 | Statistical analysis

Results are represented as the mean ± SEM. Statistical difference between groups was analyzed using SigmaStat (SPSS Science, Chicago) with parametric test one-way analysis of variance (ANOVA) followed by Dunnett's test or by non-parametric test (Kruskal–Wallis). *P* values less than .05 were considered statistically significant.

3 | RESULTS

3.1 | Elemental and ionic contents of fine particles

The size of the vast majority of CLDS-i particles is less than 1 μm, and the average grain size is between 500 and 600 nm (Figure 1A). Lunar dust particles have multifarious morphology, usually with sharp edges. By scanning electron microscopy, it was observed that the CLDS-i simulation particle was similar to lunar dust with respect to complex morphology and sharp edges (Figure 1B).

3.2 | Effects of dust on cell differential counts

The percentage of macrophages, lymphocytes, and neutrophils in BALF were evaluated. The results were shown in Table 1. The percentage of lymphocytes in the high-dose group was significantly higher than that in the control group, and the percentage of neutrophils in the LDS-exposed groups was significantly increased. The percentage of macrophages in the LDS-exposed groups was significantly decreased. There was dose-dependent relationship between the major immune cells and LDS in different BALF samples.

3.3 | Effects of dust on cytological and biochemical assessments in BALF

In order to examine lung injury, proinflammatory factors (IL-6, TNF-α), cytotoxicity markers (LDH, AKP), and permeability markers (TP, ALB) in BALF were evaluated (Table 2). The expression levels of IL-6 and TNF-α were significantly increased in the LDS high-dose group compared with those of the control group. The expression levels of LDH

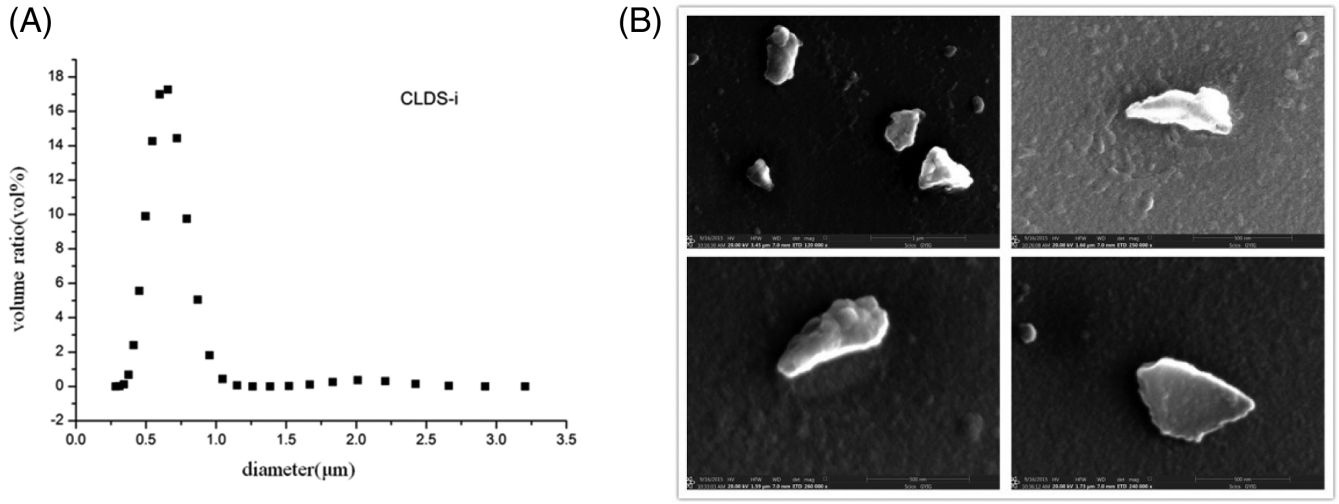

FIGURE 1 CLDS-i particle size and microscopic morphology. (A) Particle size distribution of CLDS-i. (B) Particle morphology for CLDS-i

and TP in the LDS middle- and high-dose groups were significantly higher than those of the control group. Moreover, the expression levels of AKP were significantly higher in the LDS high-dose than those in the control group. Exposure to LDS did not induce a significant difference in ALB expression compared with that in the control group, but a dose-dependent increase was observed. These results suggested that LDS exposure led to a dose-dependent upregulation in the levels of the biochemical markers in BALF. LDS exposure could cause serious toxicity, inflammation, and lung epithelial permeability.

3.4 | Pathology changes in lung tissue

To elucidate morphological alterations in the lungs, lung samples were examined by H&E and Masson's trichrome staining. The results of the H&E staining showed that pathological changes were more prominent with increasing doses of LDS (Figure 2A). Lung structures were almost normal in the control group. Slight inflammatory cell infiltration, aggregation of neutrophils, a small amount of macrophage distribution, and partial thickening of the pulmonary septum were observed in the LDS low-dose exposure group. More severe lesions were observed in the middle-dose group. Increased thickening of the pulmonary septum, aggregation of neutrophils, and the number of macrophages was observed to greater extent compared with those in the low-dose group. The most obvious lesions were observed after high-dose exposure. High levels of aggregation and infiltration of lymphocytes and neutrophils were obvious. The number of macrophages increased significantly. Interstitial cell hyperplasia was found in some areas of the lung. Alveolar structure changed significantly, even in some areas, the basic structure of the lungs remained indistinguishable.

The results of Masson's trichrome staining showed that the fibrotic lesions were enhanced along with increasing dosage of LDS (Figure 2B).The histological analysis of lung tissue showed that the treatment of the rats with LDS led to a dose-dependent increase in collagen deposition (trichrome-positive blue-colored areas) compared with that in the control group (Figure 2C). After Masson's trichrome staining is performed, the percentage of trichrome-positive tissue is calculated. There was a dose-dependent increase in fibrosis area.

The results of immunohistochemical staining showed that the positive staining for α-SMA and NOX4 in the dust-exposed groups increased significantly compared with that in the control group as shown in Figure 2D-G.

3.5 | Pulmonary oxidants and antioxidants

To explore the effects of oxidative stress on rat lung, the activities of SOD and GSH-Px, and MDA levels in lung tissues were measured (Table 3). SOD and GSH are the key antioxidant enzymes which regulate oxidative stress in cells. The activities of SOD were significantly decreased in the LDS middle- and high-dose groups, along with decreased GSH-PX expression in all LDS-exposed groups compared with levels detected in the control group. The expression levels of MDA were significantly increased in the middle- and high-dose groups compared with those in the control group.

TABLE 1 Major immune cells in the BALF after infection (n = 6)

Group	Amount of dust (mg)	Macrophages (%)	Lymphocytes (%)	Neutrophils (%)
NS	0	77.82 ± 3.80	7.50 ± 3.89	14.02 ± 3.33
LDS low-dose	0.35	68.59 ± 6.81**	9.28 ± 3.41	25.61 ± 4.83**
LDS middle-dose	1.05	61.07 ± 6.11**	12.55 ± 8.59	30.32 ± 5.21**
LDS high-dose	3.15	44.82 ± 3.81**	16.03 ± 7.30*	42.21 ± 4.02**

Note. Compared with the saline control group.
*P < .05; **P < .01.

TABLE 2 Biochemical parameters in the BALF in lung tissue after infection (n = 6)

Group	Amount of dust (mg)	AKP (IU/L)	LDH (IU/L)	ALB(g/L)	TP (g/L)	IL-6(pg/mL)	TNF-α(pg/mL)
NS	0	46.25 ± 13.50	551.42 ± 67.49	0.12 ± 0.05	0.28 ± 0.10	18.05 ± 5.69	6.24 ± 2.06
LDS low-dose	0.35	57.80 ± 12.81	567.34 ± 33.60	0.14 ± 0.15	0.20 ± 0.07	19.36 ± 10.12	8.32 ± 4.76
LDS middle-dose	1.05	58.40 ± 16.95	607.72 ± 43.26**	0.28 ± 0.16	0.36 ± 0.11*	35.72 ± 19.56	9.67 ± 5.43
LDS high-dose	3.15	72.50 ± 15.50*	652.12 ± 22.11**	0.38 ± 0.22	0.52 ± 0.16**	121.16 ± 52.11**	21.15 ± 10.86**

Note. Compared with the saline control group.
*P < .05; **P < .01.

3.6 | Expression of inflammatory pulmonary fibrosis related genes and proteins

There was a dose-dependent upregulation in iNOS gene expression, and its mRNA levels were significantly higher in the LDS high-dose group than those in the control group. The eNOS mRNA levels were significantly higher in the LDS middle- and high-dose groups. In rats that were exposed to LDS, there was a significant upregulation in NOX4 gene expression, and the levels of NOX2 mRNA were significantly higher in the high-dose group (Figure 3). These results also indicate that NOX4 is the most sensitive indicator of LDS exposure compared with eNOS, iNOS, and NOX2.

The expression levels of eNOS, iNOS, NOX2, NOX4, and α-SMA proteins were analyzed by western blotting (Figure 4). The expression of α-SMA protein as well as the levels of immunohistochemical staining for α-SMA were significantly higher in the LDS-exposed groups than in the control group (Figure 2E). The expression levels of eNOS, iNOS, NOX2, and NOX4 proteins were consistent with the levels of genes.

4 | DISCUSSION

In an effort to thoroughly investigate the pulmonary toxicity caused by lunar dust, the subacute toxicity studies are reported here. Intratracheal instillation of collected and extracted samples has limitations, including the non-physiological route of administration, which results in deposition of particle of all sizes with the same spatial distribution. However, this method is very useful if material to be studied is in very limited supply and extremely precious.[18]

It was reported that in rats exposed by inhalation to 10 mg/m^3 of either α-quartz or TiO_2 for 1 week, the lung burdens of particles were 0.72 mg quartz or 0.42 mg TiO_2. The minute respiratory volume (MRV) of a 300 g rat was 0.210 L/min.[19] Because the weight of rats (220-250 g) used in this study was similar that of rats aged 11-13 weeks,[20] if it is assumed that dust deposition in the lung is roughly proportional to the MRV of the exposed animals, the dust burden of the rat lung would also have been about 0.72 mg quartz or 0.42 mg TiO_2. Considering relative toxicity assessment and potential biological mechanisms for lunar dust, it was reasonable that a single dose of 0.35 mg per rat was chosen as a low dose, 1.05 mg as a middle dose, and 3.15 mg as a high dose in the present study. That is 0.7, 2.1, and 6.3 mg per rat for 1 week.

Another research reported that the lung burdens (determined at the end of the last exposure) of mice exposed to TiO_2 at 10, 50, or 250 mg/m^3 for 13 weeks (6 hours/day, 5 days/week) were 7.1, 45.1, and 120.4 mg/g of dry lung tissue, respectively.[21] The corresponding values for lung burden of TiO_2 per rat calculated by these authors were approximately 2.9, 18.5, and 49.4 mg (personal communication).[21] It is noteworthy that the low dose (0.35 mg/rat, 0.7 mg/week) used in our study fell between the values for lung TiO_2 burden of rats exposed to 10 mg/m^3 for 1 week (0.42 mg/rat, extrapolated above according to [20]) and those exposed to 10 mg/m^3 for 13 weeks (2.9 mg/rat). The high dose in our study (3.15 mg/rat) was comparable to the body burden of rats exposed to 50 mg/m^3 for 13 weeks in Everitt's study.[21] At the same time, these doses were not expected to cause an overdose.

An increase in neutrophils (expressed as percentage of total lavaged cells) is a biomarker for pneumonia disease. Lymphocytes are important cellular components in the immune response. The increased number of neutrophils and lymphocytes associated with pulmonary fibrosis is an indication of granulomatous and allergic reactions.[22] Although an increase in neutrophils and decrease in macrophages were also observed in all the dust-treated groups during an acute toxicity experiment,[11] the results showed more obvious pathological changes in the present report. These observations indicated that the toxic effects were gradual; thus, it took some time for neutrophils to be recruited into and accumulate significantly in the lung. In accordance with the previous research, these results suggest that it is possible to reduce lung damage caused by LDS if we can interfere with neutrophil infiltration at the early stage of lung inflammatory injury. The results indicated that in the BALF samples, there was a dose-dependent increase in AKP, ALB, TP, and LHD in the rats exposed to LDS. It reflected the extent of damage to alveolar epithelial cells and the capillary barrier. The contents of TP increased significantly in the middle- and high-dose groups due to the increased permeability of the respiratory tract mucosa, increased plasma protein contents, and increase in the release of cytoplasmic proteins as a result of lung damage. The levels of LDH increased significantly in the middle- and high-dose groups indicating type I alveolar epithelial cell damage after particulate matter entry to the trachea.[11] The inflammatory lesions in the lungs were more prominent with the increase in LDS instillation dosage in the dust exposure groups. The results of H&E staining also showed that LDS exposure could result in pathological changes in rat lungs which were consistent with the cytochemical results. It

indicated that rats exposed to LDS, to some extent, could suffer from lung injury.

IL-6 and TNF-α are pro-inflammatory cytokines. The increase in synthesis and combined effects of some pro-inflammatory regulatory factors could cause systemic inflammation.[23] TNF-α is an endothelial activation factor, which can promote the neutrophil granulocytes and eosinophil granulocytes adhered to endothelial cells, in order to facilitate their migration to inflammatory sites and enhance their toxic

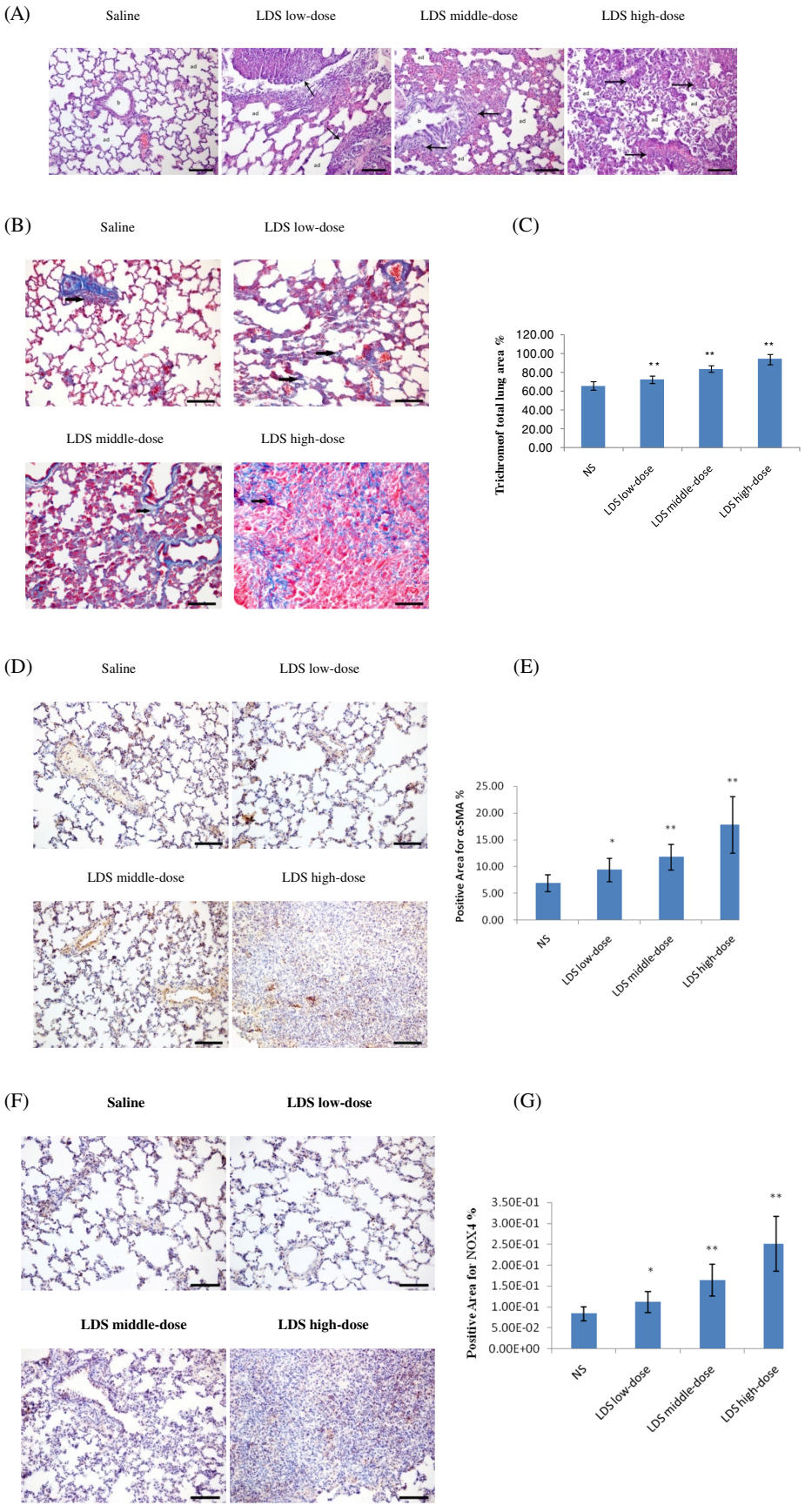

TABLE 3 Levels of SOD, GSH-PX, and MDA in lung tissue after infection (n = 6)

Group	Amount of dust (mg)	SOD (U/mg)	GSH-PX (U/mg)	MDA (mmol/mL)
NS	0	21.69 ± 2.75	102.91 ± 25.35	93.56 ± 9.09
LDS low-dose	0.35	20.22 ± 2.92	74.87 ± 15.31*	93.74 ± 11.89
LDS middle-dose	1.05	18.63 ± 2.17*	56.53 ± 13.27**	105.30 ± 23.31*
LDS high-dose	3.15	17.80 ± 3.05**	50.12 ± 19.40**	151.85 ± 15.84**

Note. Compared with the saline control group.
*P < .05; **P < .01.

effects. After being activated by the particles, macrophages, epithelium, and lymphocytes can produce IL-6 through the induction of TNF-α. In other words, TNF-α can regulate the body's inflammatory response by regulating the expression of other inflammatory factors such as IL-6, IL-1, and IL-8, and these factors further promote the progression of inflammation via TNF-α.[24] It has been shown that TNF-α could be enhanced in pulmonary artery by inhaling such particles.[25,26] TNF-α can also lead to fibroblast proliferation and collagen synthesis.[27] Therefore, it was believed that the increased TNF-α in BALF may be a sensitive early biomarker for inflammation related to pulmonary fibrosis.[28] The present results showed that the levels of TNF-α and IL-6 in the lung increased significantly in the high-dose group compared with those in the control group. It is suggested that LDS can produce inflammatory stimulation effect on lung tissue. The results of Masson's trichrome staining also supported this hypothesis. Masson's trichrome staining showed that fibrotic lesions were produced in the lungs of rats after 3 weeks of LDS exposure. Immunohistochemical staining as well as the western blotting results showed a significant increase in α-SMA expression. It indicated that fibroblasts (principle effector cells in the pathogenesis of pulmonary fibrosis) transformed to contractile myofibroblasts resulting in the formation of fibrotic foci. The results also indicated that inflammatory response was an extremely important mechanism leading to pulmonary fibrosis.

The reactive oxygen species (ROS) in the lungs can be increased by inhaled particles. Oxidative stress often occurs along with tissue inflammation, which induces the release of ROS to cause tissue injury. The free radicals induced by PM2.5 can directly act on antioxidant enzyme systems (eg, SOD, GSH, CAT) and reduce their activities.[25] MDA is the most important product of membrane lipid peroxidation, which reflects the degree of oxidative damage to the membrane system.[23] A reduction in activities of SOD and GSH-Px was found in the LDS exposure groups, and a significant increase in MDA levels suggests a large amount of ROS in the lungs. Therefore, these results indicated that the normal balance between oxidation and antioxidation was broken by LDS, which led to increased ROS levels. ROS can promote the expression of plasminogen activator inhibitor-1 (PAI-1), and overexpression of PAI-1 can lead to excessive accumulation of collagen in damaged lung tissue. Extracellular matrix (ECM) cannot degrade and eventually leads to the formation of pulmonary fibrosis.[29] At present, normal antioxidants used in clinics are not effective in the treatment of pulmonary fibrosis. Therapeutically, augmenting epithelial lining fluid glutathione in cystic fibrosis patients by means of inhalation or oral administration of the glutathione prodrug *N*-acetylcysteine is not a novel approach, but has not been clinically successful to date.[30] Therefore it indicates that more "targeted" anti-oxidative therapy should be explored for pneumonia and fibrosis.

eNOS and iNOS are nitric oxide synthase (NOS) subtypes, both expressed in vascular endothelial cells. The iNOS-derived nitric oxide (NO) has a cytotoxic effect and causes lung injury. The eNOS-derived NO has a physiological effect on healthy pulmonary functions.[31] NO is an important regulator to regulate the tension and inflammation of airway and vascular smooth muscle. It is considered that a possible mechanism of PM2.5 affecting the health is by changing nitric oxide homeostasis.[32] iNOS can be induced during the pathological state of inflammation. Exposure to fine particles can stimulate release of cytoprotective NO and upregulate iNOS messenger ribonucleic acid, while downregulating endothelial NOS suggesting that exposure to fine particles altered the NO/NOS system.[26]

Increase in iNOS levels is considered as an early indicator of the inflammatory process and abnormally expressed iNOS genes are considered as therapeutic targets for pulmonary diseases.[33] The expression of iNOS can be induced by TNF-α.[34] Our results showed that the levels of iNOS mRNA were significantly increased in the high-dose group similar to levels of TNF-α and IL-6 in lung tissue. Therefore, the increase of iNOS expression induced by LDS may be caused by these cytokines or by other mechanisms. A recent research has shown that exposure to nanotitanium dioxide particle (nTiO2) causes decreased eNOS expression and increased iNOS expression.[35] The impact of fine particles on eNOS levels is uncertain. Long-term exposure to PM contaminated air has been reported to increase the risk of developing lung disease, such as chronic obstructive pulmonary disease,[36] and chronic hypoxia can significantly increase the expression ofeNOS.[37] In

FIGURE 2 Pathology changes and Immunohistochemical staining in lung tissues. (A) Representative H&E-stained lung sections. In the figures, ad = alveolar duct, b = bronchus, and v = vessel. Lung structures were almost normal in the saline group. → = thickening of the pulmonary interstitium and presence of few inflammatory cells in the LDS low-dose group. → =significant thickening of the pulmonary interstitium and increased presence of inflammatory cells in LDS middle-dose group. → =significant thickening of the pulmonary interstitium and presence of a large number of the inflammatory cells in LDS high-dose group. (B) representative Masson's trichrome staining of lung sections. → = collagenous fiber staining can be mainly observed in the alveolar septum. (C) Trichrome stain analysis. (D) Immunohistochemical staining for α-SMA in rat lungs. (E) α-SMA immunohistochemical analysis. (F) Immunohistochemical staining for NOX4 in rat lungs. (G) NOX4 immunohistochemical analysis. Scale bars: 100 μm. The percentage of blue-colored trichrome-positive staining and the percentage of positive expression area of the lung tissues were measured with image J (12 images were taken from each group [n = 3]). The data are presented as the mean ± SD. Compared with the saline control group, *P < .05, **P < .01 [Color figure can be viewed at wileyonlinelibrary.com]

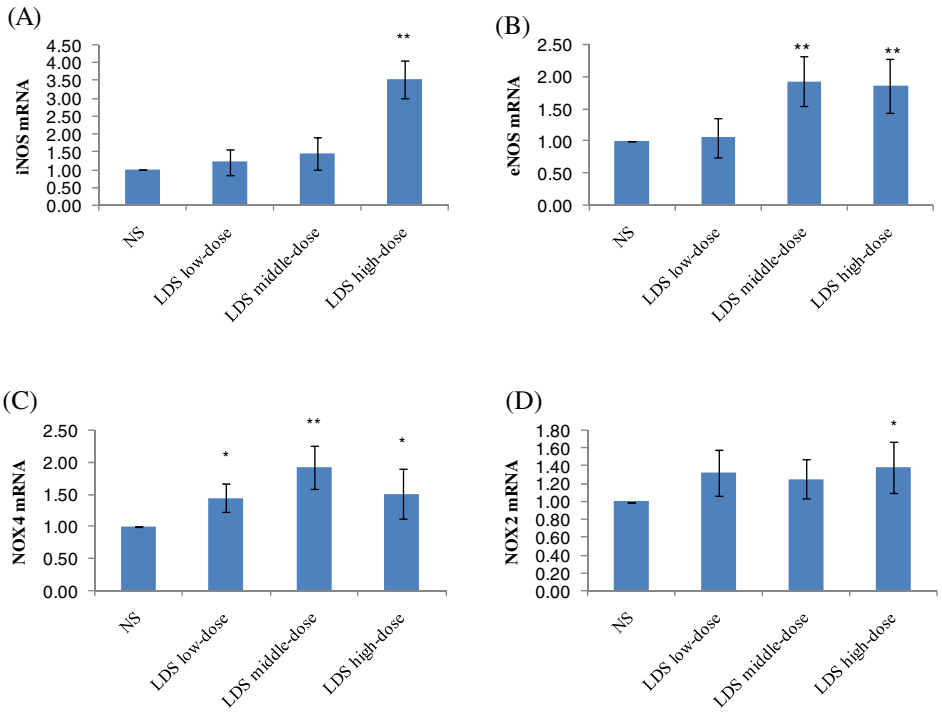

FIGURE 3 iNOS, eNOS, NOX4, and NOX2 mRNA expression in rat lungs ($n = 6$). (A) iNOS mRNA expression. (B) eNOS mRNA expression. (C) NOX4 mRNA expression. (D) NOX2 mRNA expression. The data are presented as the mean ± SD. Compared with the saline control group, $^*P < .05$, $^{**}P < .01$ [Color figure can be viewed at wileyonlinelibrary.com]

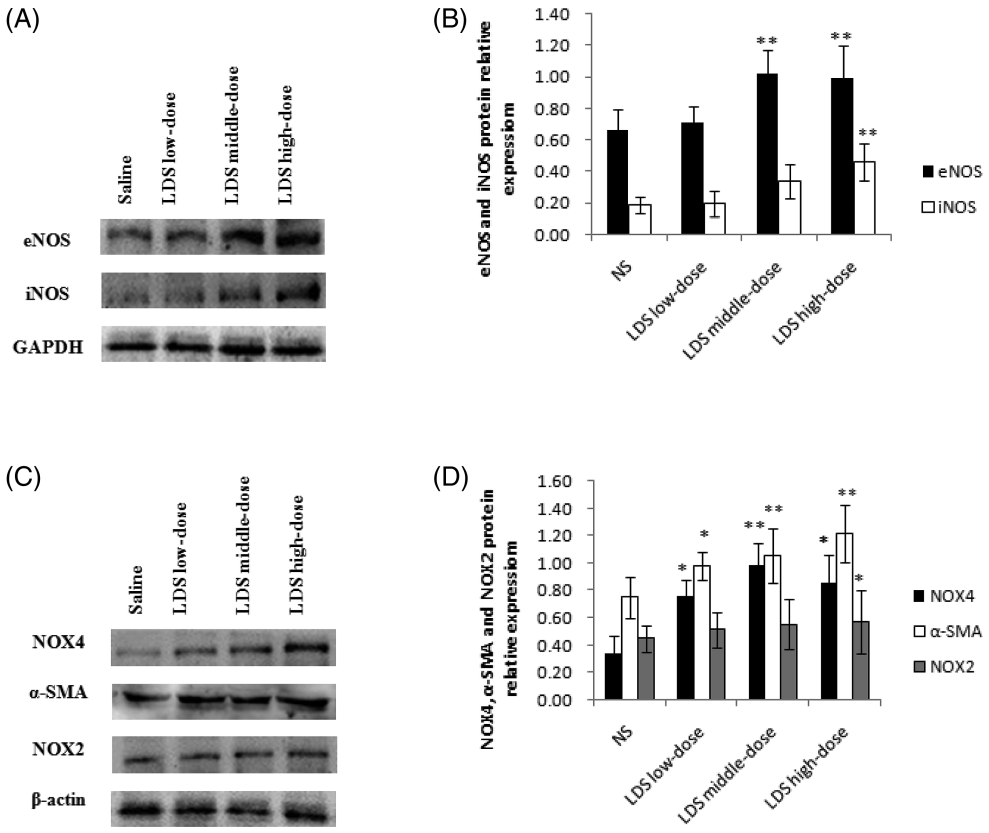

FIGURE 4 Relative expression levels of eNOS, iNOS, NOX4, NOX2 and α-SMA protein in rat lungs ($n = 3$). (A) Western blotting for eNOS and iNOS protein. (B) eNOS and iNOS protein analysis. (C) Western blotting for NOX4, NOX2 and α-SMA protein. (D) NOX4, NOX2 and α-SMA protein analysis. The final results are summarized in the bar graphs. The data are presented as the mean ± SD. β-actin and GAPDH were used as the loading control respectively. Compared with the saline control group, $^*P < .05$, $^{**}P < .01$

this study, we found that the expression of iNOS in the high-dose group was significantly increased, whereas the expression of eNOS mRNA in the middle- and high-dose exposure groups was significantly increased. We speculate that it may be because LDS particles with diameter size under 1 μm can easily cause blockage in the bronchioles and alveoli, followed by reduction in pulmonary ventilation resulting in hypoxia. Chronic hypoxia leads to increased expression of eNOS, thereby generating more endothelium NO, which may play a protective role in lung toxicity caused by LDS. This effect outweighs the negative feedback regulation of NO generated by iNOS.

NADPH oxidases are the main enzymes that produce ROS in the blood vessel. It is the most important enzyme involved in the formation of intravascular ROS, and it is also an important oxygen receptor in the body. Studies on lung inflammation using bacterial toxins, such as lipopolysaccharide (LPS), show that NADPH oxidases (NOX) regulate key inflammatory signal transduction pathways involved in lung inflammation.[38,39] Recent evidence also implicates reactive oxygen species-generating NADPH oxidase enzymes in pulmonary fibrosis, and NOX isoforms that have been reported to contribute to tissue fibrosis include NOX2[40] and NOX4.[41] NOX2 has been reported to be a major source of ROS with pulmonary inflammation. The anti-fibrotic effect of triptolide on IR-induced pulmonary fibrosis was associated with its inhibition on the axis of alveolar macrophages-NOXes-ROS-myofibroblasts.[29] NOX4 plays an important role in the pathological process of acute lung injury to fibrosis.[41] In NOX4-deficient rodent disease model, ROS generation by the NOX4 is crucial for the induction of alveolar epithelial cell death and the subsequent development of lung fibrosis.[42] The results of this study showed that LDS exposure could induce overexpression of NOX2 and NOX4 mRNA in lung tissue of rats, suggesting that the body was in oxidative stress with time after perfusion of LDS. Moreover, NOX4 is a more sensitive indicator than NOX2, and the changes in NOX4 mRNA levels are in accordance with the changes in the levels of NOX4 protein expression. Therefore, it is hypothesized that strategies aimed at specifically blocking the source of ROS ("targeted" anti-oxidative therapy) through inhibition of NOX family NADPH oxidases, especially NOX4, may prove to be more effective as anti-fibrotic therapies. The results in our study showed that exposure to LDS significantly increased the mRNA levels of NADPH oxidases indicating that subchronic exposure to LDS-induced oxidative stress adversely affects health.

Our results come with some restrictions. Firstly, toxicity, clearance, and translocation of dust in the pulmonary system are affected by their composition. Although the presence of np-Fe^0 is considered as the main factor leading to the toxicity of lunar dust, but it is in glassy rims of dust particles. It is uncertain whether this combination will decompose after entering the lung and release np-Fe^0 which causes toxicity. Metabonomics analysis is required in future research. Secondly, LDS resulted in a significant increase in eNOS levels. Although it has been shown that chronic hypoxia leads to an increase of eNOS,[37] the specific mechanism is not yet clear. Future research is needed to identify the relation between eNOS and NOX4 (a key indicator in lung fibrosis) in the rat lungs and the underlying mechanism of how they impact each other resulting in pulmonary fibrosis induced by LDS.

In summary, the treatment of the rats with LDS for 3 weeks resulted in lung lesions with significant changes in composition of immune cells and biochemical markers in the BALF. The morphological changes in lung tissue indicated that inflammatory lesions and fibrotic lesions were increased with increasing LDS dosage. Moreover, the abnormal changes in oxidative stress indicators and NADPH expression suggest that LDS may promote the development of interstitial fibrosis of the lungs by increasing oxidative stress, which promotes the inflammatory reaction. Furthermore, NOX4 is suggested to be a possible key target enzyme during pulmonary fibrosis induced by LDS. In addition, an abnormal increase in NOS suggests that LDS, which causes lung inflammation, also activates pulmonary vascular endothelial cells, impairing endothelial function. Our findings provide novel insights into the mechanism of lunar dust toxicity, which will be helpful for protecting astronauts from such toxicity during future manned lunar exploration.

ACKNOWLEDGMENT

This study was supported by the Doctoral Scientific Research Fund of Liaoning Provincial Science and Technology Department (20170520437), Open Projects Funding of Lunar and Planetary Science Laboratory, MUST—Partner Laboratory of Key Laboratory of Lunar and Deep Space Exploration, CAS (Macau FDCT grant No. 119/2017/A3), the National Science Foundation of China (51775541), the Science and Technology Development Fund (FDCT) of Macau (020/2014/A1), and the Science and Technology Research Fund of Shenyang Medical College (20171020).

CONFLICT OF INTEREST

None.

REFERENCES

1. Stubbs TJ, Vondrak RR, Farrell WM. Impact of dust on lunar exploration. *Dust Planet Syst*. 2005;643:239-243.
2. Cain JR. Lunar dust: the hazard and astronaut exposure risks. *Earth Moon Planets*. 2010;107:107-125.
3. Park J, Liu Y, Kihm KD, Taylor LA. Characterization of lunardust for toxicological studies. I: particle size distribution. *J Aerosp Eng*. 2008; 21:266-271.
4. Taylor LA, Pieters C, Patchen A, et al. Mineralogical characterization of lunar highland soils. *Lunar Planet Sci*. 2003;XXXIV:1774.
5. Keller LP, McKay DS. Discovery of vapor deposits in the lunar regolith. *Science*. 1993;261:1305-1307.
6. NASA. Constellation Program Natural Environment Definition for Design. NASA Constellation Program. NASA Document CxP70044, Revision A, National Aeronautics and Space Administration, Washington, DC. 2009.
7. Stubbs TJ, Vondrak RR, Farrell WM. A dynamic fountain model for lunar dust. *Adv Space Res*. 2006;37:59-66.
8. Darquenne C, Borja MG, Oakes JM, et al. Increase in relative deposition of fine particles in the rat lung periphery in the absence of gravity. *J Appl Physiol*. 2014;117:880-886.
9. Lam CW, James JT, McClaskey R, Cowper S, Ballis J, Muro-Cacho C. Pulmonary toxicity of simulated lunar and Martian dusts in mice: II. Biomarkers of acute responses after intratracheal instillation. *Inhal Toxicol*. 2002;14:917-928.
10. Lam CW, Scully RR, Zhang Y, et al. Toxicity of lunar dust assessed in inhalation-exposed rats. *Inhal Toxicol*. 2013;25:661-678.

11. Sun Y, Liu JG, Zheng YC, et al. Research on rat's pulmonary acute injury induced by lunar soil simulant. *J Chin Med Assoc*. 2018;81:133-140.
12. James JT, Lam CW, Santana P, et al. Estimate of safe human exposure levels for lunar dust based on comparative benchmark dose modeling. *Inhal Toxicol*. 2013;25:243-256.
13. Lam CW, James JT, McCluskey R, Cowper S, Balis J, Muro-Cacho C. Pulmonary toxicity of simulated lunar and Martian dusts in mice: I. histopathology 7 and 90 days after intratracheal instillation. *Inhal Toxicol*. 2002;14:901-916.
14. Tang H, Li X, Zhang S, et al. A lunar dust simulant: CLDS-i. *Adv Space Res*. 2016;59:1156-1160.
15. Nemmar A, Hoet PH, Dinsdale D, Vermylen J, Hoylaerts MF, Nemery B. Diesel exhaust particles in lung acutely enhance experimental peripheral thrombosis. *Circulation*. 2003;107:1202-1208.
16. Thomson E, Kumarathasan P, Goegan P, Aubin RA, Vincent R. Differential regulation of the lung endothelin system by urban particulate matter and ozone. *Toxicol Sci*. 2005;88:103-113.
17. Ghantous CM, Kobeissy FH, Soudani N, et al. Mechanical stretch-induced vascular hypertrophy occurs through modulation of leptin synthesis-mediated ROS formation and GATA-4 nuclear translocation. *Front Pharmacol*. 2015;6:240.
18. Seagrave JC, Mcdonald JD, Bedrick E, et al. Lung toxicity of ambient particulate matter from southeastern U.S. sites with different contributing sources: relationships between composition and effects. *Environ Health Perspect*. 2006;114:1387-1393.
19. Lai YL. Comparative ventilation of the normal lung. In: Parent RA, ed. *Treatise on Pulmonary Toxicology. Vol.I: Comparative Biology of the Normal Lung*. Boca Raton, FL: CRC Press; 1992:217-239.
20. Henderson RF, Driscoll KE, Harkema JR, et al. A comparison of the inflammatory response of the lung to inhaled versus instilled particles in F344 rats. *Fundam Appl Toxicol*. 1995;24:183-197.
21. Everitt JI, Mangum JB, Bermudez E, et al. Comparison of selected pulmonary responses of rats, mice, and Syrian golden hamsters to inhaled pigmentary titanium dioxide. *Inhal Toxicol*. 2000;12:275-282.
22. Mikuz G, Gschwendtner A. Value of bronchoalvoeolar lavage in the diagnosis of lung disease. *Verh Dtsch Ges Pathol*. 2000;84:129-135.
23. Sun Y, Liu JG, Kong YD, et al. Effects of lunar soil simulant on systemic oxidative stress and immune response in acute rat lung injury. *Int J Pharmacol*. 2018;14:766-772.
24. Zhang HY, Yang J, Long XN, He SH. Signal transduction pathway for TNF-induced IL-6 release from mast cells. *Chin J Cell Mol Immunol*. 2011;27:829-831.
25. Wang G, Zhao J, Jiang R, Song W. Rat lung response to ozone and fine particulate matter (PM2.5) exposures. *Environ Toxicol*. 2015;30:343-356.
26. Guo C, Xia Y, Niu P, et al. Silica nanoparticles induce oxidative stress, inflammation, and endothelial dysfunction in vitro via activation of the MAPK/Nrf2 pathway and nuclear factor-κB signaling. *Int J Nanomed*. 2015;10:1463-1477.
27. Pilling D, Vakil V, Cox N, Gomer RH. TNF-α–stimulated fibroblasts secrete lumican to promote fibrocyte differentiation. *Proc Natl Acad Sci USA*. 2015;112:11929-11934.
28. Kandhare AD, Bodhankar SL, Mohan V, Thakurdesai PA. Effect of glycosides based standardized fenugreek seed extract in bleomycin-induced pulmonary fibrosis in rats: decisive role of Bax, Nrf2, NF-κB, Muc5ac, TNF-α and IL-1β. *Chem Biol Interact*. 2015;237:151-165.
29. Chen C, Yang S, Zhang M, et al. Triptolide mitigates radiation-induced pulmonary fibrosis via inhibition of axis of alveolar macrophages-NOXes-ROS-myofibroblasts. *Cancer Biol Ther*. 2016;17:381-389.
30. Hector A, Griese M, Hartl D. Oxidative stress in cystic fibrosis lung disease: an early event, but worth targeting? *Eur Respir J*. 2014;44:17-19.
31. Davel AP, Lemos M, Pastro LM, et al. Endothelial dysfunction in the pulmonary artery induced by concentrated fine particulate matter exposure is associated with local but not systemic inflammation. *Toxicology*. 2012;295:39-46.
32. Martin W, Furchgott RF, Villani GM, Jothianandan D. Phosphodiesterase inhibitors induce endothelium-dependent relaxation of rat and rabbit aorta by potentiating the effects of spontaneously released endothelium-derived relaxing factor. *J Pharmacol Exp Ther*. 1986;237:539-547.
33. Cinar R, Gochuico BR, Iyer MR, et al. Cannabinoid CB1 receptor overactivity contributes to the pathogenesis of idiopathic pulmonary fibrosis. *JCI Insight*. 2017;2:e92281. https://doi.org/10.1172/jci.insight.92281.
34. Zheng Z, Li Z, Chen S, Pan J, Ma X. Tetramethylpyrazine attenuates TNF-α-induced iNOS expression in human endothelial cells: involvement of Syk-mediated activation of PI3K-IKK-IκB signaling pathways. *Exp Cell Res*. 2013;319:2145-2151.
35. Lee JF, Tung SP, Wang D, et al. Lipoxygenase pathway mediates increases of airway resistance and lung inflation induced by exposure to nanotitanium dioxide in rats. *Oxid Med Cell Longev*. 2015;2014:485604.
36. Kermani M, Fallah Jokandan S, Aghaei M, et al. Estimation of cardiovascular death, myocardial infarction and chronic obstructive pulmonary disease (COPD) attributed to PM and SO2 in the air of Tehran metropolis. *J Res Environ Health*. 2016;2:116-126.
37. Zhang E, Maruyama J, Yokochi A, et al. Sarpogrelate hydrochloride, a serotonin 5HT2A receptor antagonist, ameliorates the development of chronic hypoxic pulmonary hypertension in rats. *J Anesth*. 2015;29:715-723.
38. Han W, Li H, Cai J, et al. NADPH oxidase limits lipopolysaccharide-induced lung inflammation and injury in mice through reduction-oxidation regulation of NF-κB activity. *J Immunol*. 2013;190:4786-4794.
39. Cho RL, Yang CC, Lee IT, et al. Lipopolysaccharide induces ICAM-1 expression via a c-Src/NADPH oxidase/ROS-dependent NF-κB pathway in human pulmonary alveolar epithelial cells. *Am J Physiol Lung Cell Mol Physiol*. 2016;310:L639-L657.
40. Menden HL, Xia S, Mabry SM, Navarro A, Nyp MF, Sampath V. Nicotinamide adenine dinucleotide phosphate oxidase 2 regulates LPS-induced inflammation and alveolar remodeling in the developing lung. *Am J Respir Cell Mol Biol*. 2016;55:767-778.
41. Guo W, Saito S, Sanchez CG, et al. TGF-β1 stimulates HDAC4 nucleus-to-cytoplasm translocation and NADPH oxidase 4-derived reactive oxygen species in normal human lung fibroblasts. *Am J Physiol Lung Cell Mol Physiol*. 2017;312:L936-L944.
42. Jarman ER, Khambata VS, Cope C, et al. An inhibitor of NADPH oxidase-4 attenuates established pulmonary fibrosis in a rodent disease model. *Am J Respir Cell Mol Biol*. 2014;50:158-169.

How to cite this article: Sun Y, Liu J, Zhang X, Li X, Zhou B, Lv Z. Mechanisms involved in inflammatory pulmonary fibrosis induced by lunar dust simulant in rats. *Environmental Toxicology*. 2019;34:131–140. https://doi.org/10.1002/tox.22665